Pergamon

Tetrahedron, Vol. 53, No. 13, pp. 4947-4956, 1997

0040-4020/97 $17.00 + 0.00

PII: S0040-4020(97)00189-0

ESR Study of Thianthrenium Radical Cation within Acid Zeolites

José-Vicente Folgado,[1] Hermenegildo García,*[2] Vicente Martí[2] and Mercedes Esplá[2]

[1] UIBCM-Departament de Química Inorgànica, Universitat de València, Dr. Moliner 50, 46100-Burjasot, València, Spain

[2] Instituto de Tecnología Química CSIC-UPV and Departamento de Química, Universidad Politécnica de Valencia, Apartado 22012, 46071-Valencia, Spain; e-mail address: hgarcia@vega.cc.upv.es

Abstract. Thianthrene (E_{ox} = 1.47 V *vs* NHE) has been adsorbed into a series of zeolites beta (ß) and ZSM-5 in the NH_4^+ or H^+ forms, having different particle size and Si/Al ratio. The resulting population of generated thianthrenium radical cation was determined by a combination of diffuse reflectance and ESR spectroscopies. From the results obtained it can be concluded: i) the process takes predominantly place in the interior of the voids (XPS measurements and lack of influence of the particle size); ii) ZSM-5 is more efficient than zeolite ß; iii) no strong acid sites are required (both NH_4^+ and H^+ forms produced very similar spin concentrations); iv) the zeolite framework acts isolating the organic spins, thus avoiding diamagnetic coupling (zeolite samples do obey Curie law); and v) the population of oxidizing sites increases with the aluminum content of the zeolite.

INTRODUCTION

Formation of radical cations as persistent intermediates by mere adsorption of electron-rich organic molecules onto zeolites is a well-documented process,[1-8] which is, however, not fully understood.[9] Zeolites are microporous crystalline aluminosilicates[10-12] of different structures, whose physicochemical parameters and chemical composition can be modified by synthesis as well as by post-synthetic treatments.[13] There are more than 300 different zeolites synthesized so far and this offers the possibility to choose among a wide range of different geometries and dimensions of the internal voids. In cases in which a tight fit between the framework of the zeolite and the molecular dimensions of the guest occurs, it has been observed that organic radical cations can survive as indefinetely stable species. Therefore, zeolites appear as a convenient media to characterize and determine the molecular properties of organic radical cations.

Recently, using thianthrene (TH, E_{ox}=1.47 V vs NHE[14, 15]) as a probe, we have shown that there is a clear relationship between the presence of acid sites and the ability of zeolites to generate the corresponding $TH^{+\bullet}$ radical cation.[16] TH forms one of the best-documented radical cation in the liquid phase and a great deal of information is available concerning its characterization, physical properties and chemical behavior.[17-21]

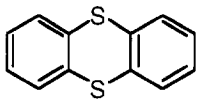

TH

Our previous report was focused on the characterization of the TH-HZeol systems and was mainly based on diffuse reflectance spectra. While this technique gave valuable information concerning formation, decay and aggregation of $TH^{+\bullet}$, no direct evidences concerning its location (internal *versus* external surface of the particles), population and coupling between neighbour spins was obtained. Circumstancial evidences based on reaction products indicated that the ability of zeolites in their H^+-form to generate $TH^{+\bullet}$ was at least three orders of magnitude higher than previous estimates based on ESR measurements on other Na^+ containing samples.[6] In the present work, we have performed a quantitative estimate of the absolute spin concentration for this type of TH-HZeol composites by means of a combination of ESR and diffuse reflectance spectroscopies. Our results show that values almost reaching 10^{20} spins$\bullet g^{-1}$ can be easily generated by adsorption on acid zeolites. In addition, we have supported the internal location of $TH^{+\bullet}$ by XPS spectroscopy and established that $TH^{+\bullet}$ embedded within the zeolite framework behaves as isolated spins in contradistinction with samples of the same radical cation in homogeneous media where diamagnetic coupling between spin pairs occurs.

RESULTS AND DISCUSSION

Two types of zeolites, ZSM-5 and beta (ß), having different structure and topology were used in this study.[22] The former is a medium pore zeolite of the pentasil family whose structure is formed by two interconnected systems of channels (straight 5.2 x 5.7 Å, sinusoidal 5.3 x 5.6 Å), crossing at right angles. ß is a tridirectional large pore zeolite comprising oval-shaped cavities of an approximate maximum length of 12 Å. The zeolite samples also differ in their aluminum content and crystallite particle size. They were used in the H^+ as well as in the NH_4^+ forms. The main physicochemical parameters of the zeolites used in this work are summarized in Table 1.

Adsorption of TH was carried out in the vapor phase by heating progressively to 175 ^oC under continuous flow of inert gas an intimate mixture of TH and zeolite powders, without prior dehydration of the zeolite. Previous studies by thermogravimetric analysis for the NH_4^+-exchanged samples established that no appreciable decomposition of this ion takes place below 200^oC. Formation of $TH^{+\bullet}$ was ascertained by diffuse reflectance spectroscopy of the composites and by IR spectroscopy.[16] The final content of organic material retained on the composites was established for all the samples by combustion elemental analysis (C and S) and was always significantly lower than the initial amount of TH added prior to the incorporation. This indicates that partial sublimation of TH out of the system takes place during the incorporation procedure. As a general rule, large pore zeolite ß incorporates much larger amounts than medium pore ZSM-5. X-Ray diffraction of the powders established that the incorporation procedure leads to the total disappearance of the TH crystals. All these facts indicate that incorporation of TH into the solids takes places from the vapor phase and that the amount of TH included is primarily related to the pore volume of the zeolite (ß samples retaining larger amounts

than ZSM-5). Table 2 summarizes some of the spectroscopic and gravimetric properties of the composites. After their preparation, the samples remained unaltered for periods exceeding several months under usual laboratory conditions, as evidenced by the absence of detectable changes in the diffuse reflectance and ESR spectra.

Zeolite	Si/Al Molar Ratio†	Crystal Size (μm)	BET Surface Area ($m^2 \times g^{-1}$)	Micropore Volume ($ml \times g^{-1}$)
ZSM-5-a	17.5	1 - 3	380	0.1136
ZSM-5-b	26.5	1 - 3	390	0.1236
ZSM-5-c	37.5	1 - 3	390	0.1122
ZSM-5-P	20	0.1	--	--
Silicalite	-‡	1-3	380	0.1128
Hß-a	13	0.15	666	0.1889
Hß-b	17	0.06	--	0.1809
Hß-c	17	0.35	583	0.1870
Hß-d	15	0.6	533	0.2130

† Measured by chemical analysis; ‡ no framework Al is present.

Table 1. Relevant characteristics of the zeolites used in this work

Concerning the location of TH (internal voids *versus* external surface), we addressed the possibility that, especially in the case of medium pore ZSM-5, TH was only present on the external surface of the particles. In order to disclose this question, the most general methodology consists of studying samples with very similar physicochemical parameters, but with different crystallite size. A decrease in the average particle diameter increases the ratio of external versus internal surface area and, therefore, samples with smaller crystallite dimensions should produce larger populations of $TH^{+\bullet}$ if only the external surface were involved in the process. As can be seen in Table 2, neither the total amount of adsorbed organic material or the number of spins per gram of zeolite increases as the size of the particles decreases (compare entries 8 and 11 that correspond to zeolites with the smaller particle size). This observation strongly indicates that the generation of $TH^{+\bullet}$ takes mainly place inside the micropores of the solids. Furthermore, XPS analysis of the external surface of a sample of TH adsorbed into silicalite did not show a measurable presence of carbon or sulphur atoms. Only after intensive Ar^+ sputtering that produce the decapping of the outermost layers of the zeolite grains we were able to detect the presence of TH along with the Si and O of the lattice. This constitutes firm evidence that TH is embedded within the zeolite micropores.

In a number of cases (entries 1, 2, 4, and 7 in Table 2, see also Figure 1), the samples only contained pure $TH^{+\bullet}$ as evidenced by (i) the lack in the UV of the 260 nm band characteristic of neutral TH, and (ii) the absence of the 1550 cm^{-1} vibration in the aromatic region of the IR spectra owing to TH. For these samples, the amount of $TH^{+\bullet}$ must correspond to the total content in organic material. These values were used to perform

the absolute calibration of the ESR signal area. In contrast, non-acidic zeolites such as silicalite (entry 9 in Table 2) do not generate appreciable amounts of $TH^{+\bullet}$ as evidenced by the DR and ESR spectra. This result confirms

Entry	Zeolite	Charge balancing cation	Organic material† (mg TH/g zeolite)	Ratio $TH^{+\bullet}$/TH (540/260 nm)‡	Loading level TH/H^+,NH_4^+ (%)	Spin x 10^{-18} / g zeolite
1	ZSM-5-a	H^+	9.4	§	5.4	42
2	ZSM-5-b	H^+	9.6	§	8.2	42
3	ZSM-5-c	H^+	7.9	0.7	9.4	7
4	ZSM-5-a	NH_4^+	12.0	§	10.2	50
5	ZSM-5-b	NH_4^+	9.0	1.3	7.6	11
6	ZSM-5-c	NH_4^+	8.5	0.6	10.1	4
7#	ZSM-5-a	NH_4^+	9.3	§	5.3	42
8	ZSM-5-P	H^+	5.7	1.1	3.7	7
9	Silicalite	none	5.0	0	--	<0.2
10	Hß-a	H^+	57.2	0.6	25.8	6
11	Hß-b	H^+	54.6	0.8	23.6	14
12	Hß-c	H^+	56.4	0.7	24.4	32
13	Hß-d	H^+	59.7	0.45	24.7	6

† measured by combustion elemental analysis (C, S); ‡ intensity ratio of the characteristic absorption bands (TH 260, $TH^{+\bullet}$ 540 nm) in the diffuse reflectance spectra of the samples; § the 260 nm band of neutral TH was absent; # adsorption carried out using half amount of TH.

Table 2. Loading levels and relevant spectroscopic properties of $TH^{+\bullet}$-HZeol samples.

that the presence of a high population of oxidizing sites in the zeolite is related with the presence of acid sites as it has been previously reported.[16]

In fact, all the studied samples except silicalite showed at room temperature a very similar ESR spectrum consisting of an intense, broad, three-components signal. A representative example is given in Figure 2. The corresponding g-values were g_1= 2.012, g_2= 2.007, and g_3= 2.002 ($g_{average}$= 2.007). In the central part of the spectrum a five line hyperfine structure can be observed in some samples (better resolved at low temperatures, see Figure 2), with a mean separation of 1.3 Gauss. All these features are obviously attributed to

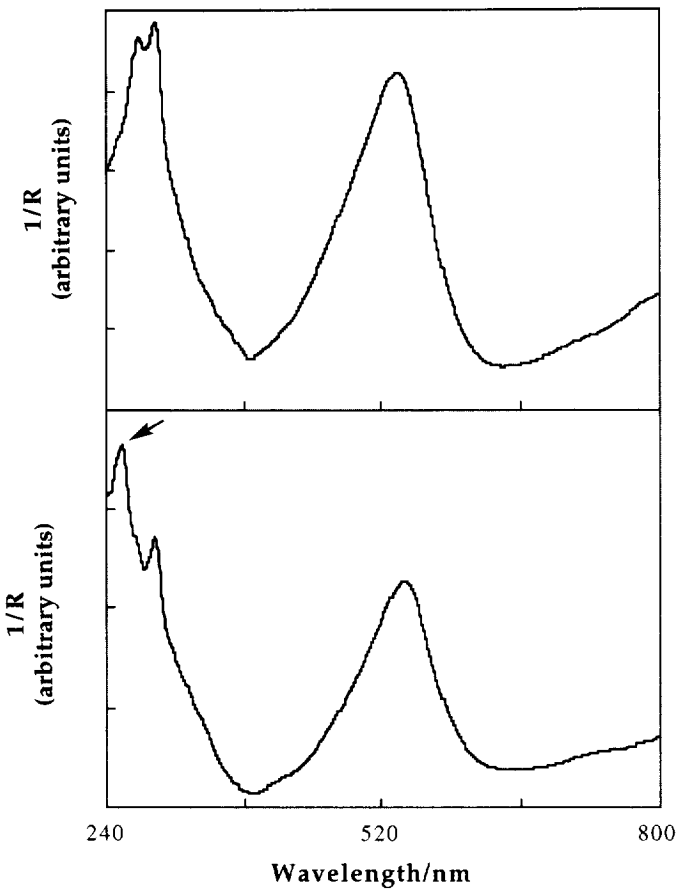

Figure 1. Diffuse reflectances (1/R) of TH-HZSM-5-a (upper curve) and TH-Hß-c (lower spectrum) samples. While in the first spectrum a doublet corresponding to pure $TH^{+\bullet}$ is observed in the UV region, the second one exhibits a band at 260 nm (marked with an arrow) owing to neutral TH.

the presence of the $TH^{+\bullet}$ cation radical in the samples.[18, 23] The total area of the full signal was obtained by double integration of the spectra and reduced by taking into account the sample mass and the spectrometer gain conditions. These data are also collected in Table 2 and allowed the determination of spin concentration for the rest of the samples containing $TH/TH^{+\bullet}$ mixtures (estimated error 15%).

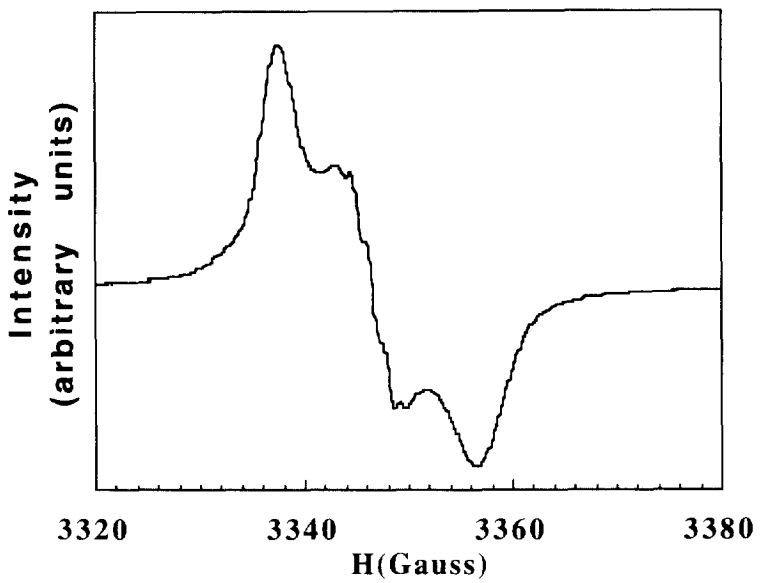

Figure 2. ESR spectrum (v=9.40 GHz) of TH-Hß-a sample recorded at 120 K.

Concerning the interpretation of the observed ESR signals, several remarks must be made. Thus, by treating the samples with concentrated sulfuric acid (96%), a purple solution is obtained. Its EPR spectrum, recorded at room temperature in the liquid phase (Figure 3, spectrum a), consists of a quintuplet (approximate intensity ratios of 1:4:6:4:1, A=1.3 Gauss) centered at g= 2.008. This corresponds to the well established hyperfine coupling from the 2, 3, 7 and 8 protons of the $TH^{+\bullet}$.[23] Upon lowering the temperature of the solution, it becomes progressively blue and the ESR spectrum (solid phase) broadens (Figure 3, curve c), and eventually disappears below 120 K.

We have observed similar results for solid $TH^{+\bullet}BF_4^-$ in good agreement with previous reports about the solid state ESR spectra of this and other THX salts (X=ClO_4, $SbCl_5$).[18] In fact, the room temperature, solid state ESR spectra of these salts consist of a broad three lines pattern as that shown in Figure 3b. The signals are of weak intensity that diminish on lowering the temperature and practically vanish below 120 K. This is consistent with the formation of dimers $(TH^{+\bullet})_2$ with strong antiferromagnetic coupling, as it was pointed earlier by Lucken.[18]

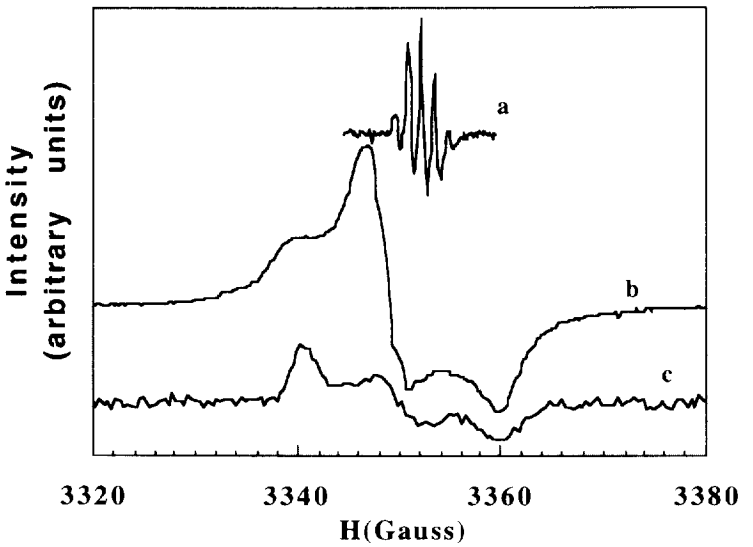

Figure 3. ESR spectra (v=9.41 GHz) of: a) sulfuric acid extract from $TH^{+\bullet}$-Hß-a sample recorded at room temperature (liquid phase); b) solid $THBF_4$ at room temperature; c) same extract as spectrum a, but recorded at 210 K (solid). Spectra have been shifted in the intensity axis.

In sharp contrast, the intensity of the spectra of $TH^{+\bullet}$ embedded in zeolite increase upon lowering the temperature and follows approximately a Curie law. This can be interpreted as experimental evidence for the presence of isolated paramagnetic $TH^{+\bullet}$ radicals, the zeolite framework acting as a rigid, insulating matrix. When these radical cations are formed, they are hold in the zeolite holes and anisotropic spectra result (Figure 2), different to the isotropic ones observed in homogeneous phase. This kind of anisotropic spectra has been observed in other sulfur-containing radicals in the solid state,[24, 25] and also in photoirradiated samples of thianthrene adsorbed on clay surfaces.[26] The anisotropy and the mean g-value larger than 2.0023, are essentially due to the high spin density on the sulfur atoms.[23-25]

Both NH_4^+ and H^+ forms of zeolites are apparently capable to generate the same amount of $TH^{+\bullet}$, in spite of their very different acid strength. This result fits well with previous findings that no strong acid sites are necessary to generate radical cations.[16, 27]

On the other hand, the ZSM-5 series expands on a range of framework Si/Al ratios wide enough to establish that a higher aluminum content favors higher concentrations of $TH^{+\bullet}$, both in the NH_4^+ or H^+ forms. Thus, the amount of radical cations that could be generated in the ZSM-5 with the lower aluminum content (entries 3 and 6) is comparatively lower than that of the two other samples with the same crystalline structure.

This fact is rather surprising taking into account that the population of Brönsted acid sites for this dealuminated ZSM-5-c (Si/Al 37.5), although lower than for the other samples with higher aluminum content, is still one order of magnitude higher the amount of adsorbed TH (see $TH^{+\bullet}/H^{+}$ ratio in Table 2). However, in spite of this large excess of H^{+}, attempts to obtain higher $TH^{+\bullet}/H^{+}$ ratios were unsuccessful. This would indicate that not all the acid sites can intervene as electron acceptors, but only a small fraction of them (about one tenth maximum). However, it is generally assumed that all the Brönsted sites present on highly dealuminated samples possess the same acid strength; that is: these centers formed by bridging Si(OH)Al hydroxyl groups are all uniform from the point of view of their chemical composition (i.e. number of aluminum in the second coordination sphere) and acid strength.[28] Clearly, no differences on the sites should be expected if the oxidizing ability would parallel strictly the acid properties of the sites.

In this context, it is clear that the very different particle size of ZSM-5-P and the other ZSM-5 samples precludes a direct comparison between them based exclusively on the effect of the framework Si/Al ratio. Thus, the amount and location of the adsorbed guests varies due to differences in the ratio of the external *versus* internal surface areas.

Another effect that remains to be understood is the influence of the crystalline structure on the electron acceptor ability of zeolites. Thus, results of Table 2 reveal that medium pore ZSM-5 is far more efficient than large pore ß zeolites with similar physicochemical parameters. This would indicate that besides their chemical composition, confinement of TH and the sites in a tight fit, closed reaction cavity plays a determinant role in this

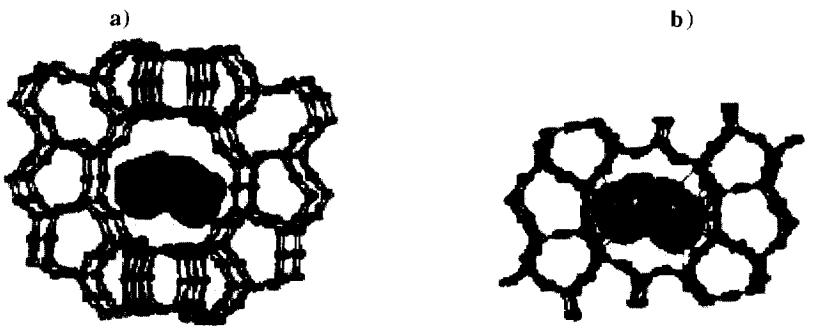

Figure 4. Docking of TH within zeolite ß (a) and ZSM-5 (b) using Insigth II molecular modeling package programs running on a Silicon Graphics work station. The view corresponds to a cross section perpendicular to the axis of the channels. While no van der Waals interactions are predicted for TH inside large pore size zeolite ß, the lines connecting TH and medium pore size ZSM-5 framework show a severe overlapping of host-guest atomic radii.

process. Recent calculations on the variation of the HOMO energy (and therefore the ionization potential) owing to possible orbital deformations when a molecule is placed in a restricted space would provide a theoretical basis to rationalize this phenomenon.[29]

Figure 4 visualizes the docking of TH in the cages of ß and ZSM-5 zeolites and shows the strong van der Waals overlap in the latter case. Furthermore, it is known that while the geometry of neutral TH is not

planar and shows a dihedral angle of 128°, the corresponding radical cation is considerably more planar (interplanar angle between the benzo rings of 174°).[30] Molecular modeling predicts that after generation of $TH^{+\bullet}$ the overlapping between host/guest atoms in the case of ZSM-5 would slightly increase if planarity of the rings is achieved.

CONCLUSIONS

We have shown that high concentrations of radical cations (about 10^{20} spin•g^{-1}) can be formed during the incorporation of electron-rich organic molecules such as TH into the H^+ or NH_4^+-forms of zeolites. Thus, samples containing pure radical cation have been obtained. In contrast, non-acidic silicalite is totally unable to generate $TH^{+\bullet}$. Compared with other solid $TH^{+\bullet}$ salts, the zeolite framework acts insulating molecular spins, thus avoiding antiferromagnetic radical cation aggregation. About 10% of the acid sites have found to be active to generate $TH^{+\bullet}$. Influence of the crystallite particle size on the spin concentration established that this process mainly occurs in the internal voids of the zeolites. As previously reported, a clear relationship between the aluminum content (i.e. number of acid sites) and oxidizing activity has been observed. Crystalline structure of the zeolite is also an important factor, ZSM-5 being more efficient than zeolite ß.

EXPERIMENTAL

TH was purchased from Aldrich and used as received. Zeolites ZSM-5-a, ZSM-5-b, and ZSM-5-c were supplied by PQ in their NH_4^+ form. Their H^+-form was obtained by ammonium decomposition calcining overnight at 500°C. Zeolite ZSM-5-P with small average crystal size was synthesized following reported procedures.[31] Zeolites ß with different crystallite size were prepared by decomposition of the tetraethylammonium forms of as-synthesized samples prepared according to the literature.[32] Average particle size was determined by SEM following the ASTM protocol. Surface areas were determined after calcination using a Micromeritcs equipment. UV/Vis diffuse reflectances were recorded in a Shimadzu UV-2101 PC scanning spectrophotometer provided with an integrating sphere. IR spectra were obtained using a Nicolet 710 FT-IR spectrophotometer in self-consistent wafers (10 mg) after outgassing at 200°C and 10^{-2} Pa for 1 h. ESR were recorded on a Brucker ER 200D spectrometer equipped with a variable temperature device at X-band (9.4-9.8 GHz) and using DPPH (g=2.0036) as standard reference. XPS spectrum of TH incorporated on silicalite was obtained with a VG-Escalab 210 spectrometer equipped with Mg anode (K_α=1253.6 eV) operated at 240 W (12 Kv and 20 mA). The residual pressure in the analysis chamber was maintained lower than 5 x 10^{-9} mbar. Wafered samples were attached onto a stainless steel sample holder. Binding energies were scaled against C(1s) peak (284.6 eV).

Adsorption of TH (35 mg) onto zeolites (500 mg) without any pretreatment was accomplished by thoroughly grinding both solids in a mortar at room temperature and heating the mixture in a oven progressively (5 °C • min^{-1}) up to 175 °C under Ar flow (20 ml x min^{-1}).

$THBF_4$ was prepared from TH by treatment with $NOBF_4$ (Aldrich used as received) in dry acetonitrile following the procedure reported in the literature.[21] Purity of $THBF_4$, established by iodometric titration, was 83%.

ACKNOWLEDGEMENTS

Financial support of the Spanish DGICYT (grant no PB93-0380), the Generalitat Valenciana (fellowship to V.M.) and partially by the European Comission within the Program of Human Capital and

Mobility (CHRX-CT93-0280) are acknowledged. Thanks are due to R. Torrero and M. Tadeo for technical assistance.

REFERENCES

1. Chen, F.R.; Fripiat, J.J., *Ninth International Zeolite Conference*. **1992**, I, 603-610.
2. Rhodes, C.J., *Coll. Surf. A* **1993**,*72*, 111-118.
3. Rhodes, C.J.; Reid, I.D.; Roduner, E., *J. Chem. Soc., Chem. Commun.* **1993**,512-513.
4. Chen, F.R.; Fripiat, J.J., *J. Phys. Chem.* **1993**,*97*, 5796-5797.
5. Ramamurthy, V.; Eaton, D.F.; Caspar, J.V., *Acc. Chem. Res.* **1992**,*25*, 299-306.
6. Ramamurthy, V.; Caspar, J.V.; Corbin, D.R., *J. Am. Chem. Soc.* **1991**,*113*, 594-600.
7. Caspar, J.V.; Ramamurthy, V.; Corbin, D.R., *J. Am. Chem. Soc.* **1991**,*113*, 600-610.
8. Ramamurthy, V., *Chimia* **1992**,*46*, 359-376.
9. Rhodes, C.J. Electron Spin Resonance. *Annual Reports on the Progress of Physical Chemistry*. 1993 Royal Society of Chemistry. London.
10. Breck, D.W. *Zeolite Molecular Sieves: Structure, Chemistry and Use*; John Wiley and Sons: New York, 1974.
11. Dyer, A. *An Introduction to Zeolite Molecular Sieves*; John Wiley & Sons: Bath, U. K., 1988.
12. *Introduction to Zeolite Science and Practice*, van Bekkum, H.; Flanigen, E.M.; Jansen, J.C. ed., Elsevier: Amsterdam, 1991.
13. *Zeolites and Related Microporous Materials: State of the Art 1994*, Weitkamp, J.; Karge, H.G.; Pfeifer, H.; Hölderich, W. ed., Elsevier: Amsterdam, 1994.
14. Jones II, G.; Huang, B., *Tetrahedron Lett.* **1993**,*34*, 269-272.
15. Jones II, G.; Huang, B.; Griffin, S.F., *J. Org. Chem.* **1993**,*58*, 2035-2042.
16. Corma, A.; Fornés, V.; García, H.; Martí, V.; Miranda, M.A., *Chem. Mater.* **1995**,*7*, 2136-2143.
17. Fava, A.; Sogo, P.B.; Calvin, M., *J. Amer. Chem. Soc.* **1957**,*79*, 1078-1083.
18. Lucken, E.A.C., *J. Chem. Soc.* **1962**,4963-4965.
19. Shine, H.J.; Piette, L., *J. Am. Chem. Soc.* **1962**,*1963*, 4798-4806.
20. Murata, Y.; Shine, H.J., *J. Org. Chem.* **1969**,*34*, 3368-3372.
21. Boduszek, B.; Shine, H.J., *J. Org. Chem.* **1988**,*53*, 5142-5143.
22. Meier, W.M.; Olson, D.H. *Atlas of Zeolite Structure Types*; Butterworths: London, 1992.
23. Shine, H.J.; Dais, C.F.; Small, R.J., *J. Org. Chem.* **1964**,*29*, 21-25.
24. Kinoshita, M., *Bull. Chem. Soc. Jpn.* **1962**,*35*, 1137-1140.
25. Kurita, M.; Gordy, W., *J. Phys. Chem.* **1961**,*34*, 1285.
26. Mao, Y.; Thomas, J.K., *J. Org. Chem.* **1993**,*58*, 6641-6649.
27. Cano, M.L.; Corma, A.; Fornés, V.; García, H., *J. Phys. Chem.* **1995**,*99*, 4241-4246.
28. Pine, L.A.; Maher, P.J.; Watcher, W.A., *J. Catal.* **1984**,*85*, 446.
29. Zicovich-Wilson, C.; Planelles, J.H.; Jaskolski, W., *Int. J. Quantum Chem.* **1994**,*50*, 429-444.
30. Bock, H.; Rauschenbach, A.; Näther, C.; Kleine, M.; Havlas, Z., *Chem. Ber.* **1994**,*127*, 2043-2049.
31. Argauer, R.J.; Landlolt, G.R., *U.S. Pat.* **1982**,3 702 886.
32. Camblor, M.A.; Mifsud, A.; Pérez-Pariente, J., *Zeolites* **1991**,*11*, 792-797.

(*Received in UK* 13 *January* 1997; *accepted* 20 *February* 1997)